J. Biol. Chem. 253, 6946–6954.
Meyer, W. L., & Meyer, R. B. (1963) J. Am. Chem. Soc. 85, 2170–2171.
Murphy, L. M., Ellison, R. R., Karnofsky, D. A., & Burchenal, J. H. (1954) J. Clin. Invest. 33, 1388.
Roth, B., & Cheng, C. C. (1982) Progr. Med. Chem. 19, 270–331.
Tendler, S. J. B., Griffin, R. J., Birdsall, B., Stevens, M. F. G., Roberts, G. C. K., & Feeney, J. (1988) FEBS Lett. 240, 201–204.
Wider, G., Macura, S., Kumar, A., Ernst, R. R., & Wuthrich, K. (1984) J. Magn. Reson. 45, 207–234.
Williamson, M. P., Marion, D., & Wuthrich, K. (1984) J. Mol. Biol. 173, 341–359.

Partial ^{1}H NMR Assignments of the *Escherichia coli* Dihydrofolate Reductase Complex with Folate: Evidence for a Unique Conformation of Bound Folate†

Christopher J. Falzone,‡ Stephen J. Benkovic,*,‡,§ and Peter E. Wright*,§

Department of Chemistry, The Pennsylvania State University, 152 Davey Laboratory, University Park, Pennsylvania 16802, and Department of Molecular Biology, Research Institute of Scripps Clinic, 10666 North Torrey Pines Road, La Jolla, California 92037

Received April 16, 1990; Revised Manuscript Received July 11, 1990

ABSTRACT: Sequence-specific ^{1}H assignments have been made for over 25% of the amino acid side chains of *Escherichia coli* dihydrofolate reductase complexed with folate by using a variety of two-dimensional techniques. Proton resonances were assigned by using a combination of site-directed mutagenesis and a knowledge of the X-ray crystal structure. Unique sets of NOE connectivities present in hydrophobic pockets were matched with the X-ray structure and used to assign many of the residues. Other residues, particularly those near or in the active site, were assigned by site-directed mutagenesis. The ability to assign unambiguously the proton resonances of these catalytically important residues allowed for extensive networks of NOE connectivities to follow from these assignments. As a consequence of these assignments, the orientation of the pterin ring of folate could be determined, and its conformation is similar to that of the productive dihydrofolate complex. Under these experimental conditions, only one bound form of the pterin ring could be detected.

Dihydrofolate reductase (5,6,7,8-tetrahydrofolate:NADP$^+$ oxidoreductase, EC 1.5.1.3) is a monomeric protein consisting of 159 amino acids and has a molecular mass of 18 000 daltons. This enzyme catalyzes the NADPH-dependent reduction of 7,8-dihydrofolate (H_2F)[1] to 5,6,7,8-tetrahydrofolate (H_4F) and is responsible for maintaining intracellular levels of H_4F. Tetrahydrofolate and its derivatives are essential cofactors in one-carbon transfer reactions in a number of biosynthetic pathways. Thus, dihydrofolate reductase (DHFR) is an important target enzyme for antifolate drugs such as the antitumor agent methotrexate (MTX) and the antimicrobial agent trimethoprim.

The crystal structure for DHFR from *Escherichia coli* with the inhibitor MTX bound has been determined to a resolution of 1.7 Å (Bolin et al., 1982). It shows an abundance of secondary structure including four helices and an eight-stranded β-sheet. In comparing DHFR from *E. coli* to enzyme from other sources, it is observed that the secondary and tertiary structures are similar despite low primary sequence homology. For example, DHFR from *Lactobacillus casei* and *E. coli* share only a 28% primary sequence homology. However, some residues are strictly conserved or semiconserved (Glu for Asp substitution, for example), and when active site homology is compared, as many as 70% of the residues fall into these two categories for the NADPH site in the *L. casei–E. coli* comparison (Benkovic et al., 1988). Thus, there are certain key residues that occur in all species that have been optimized, at least under cellular conditions, for binding and catalysis. The role of these amino acids has been studied by combining site-directed mutagenesis with a detailed kinetic analysis in order to learn more about the relationship between structure and function.

The kinetic schemes for wild-type and several mutant DHFR's have been derived from pre-steady-state and steady-state kinetics (Fierke et al., 1987; Fierke & Benkovic, 1989; Murphy & Benkovic, 1989). Despite this detailed knowledge of the kinetic steps in the mechanism of DHFR and a knowledge of the stereochemistry of the reduction of dihydrofolate (Charlton et al., 1979), no other information is available about the structures of the substrates in the active sites of wild-type and mutant proteins and how these structures are related to the kinetic mechanism. We have begun to apply two-dimensional NMR methods to obtain information about the structure of the active site in *E. coli* DHFR and various

† This work was supported by National Institutes of Health Grants GM 24129 to S.J.B. and GM 36643 to P.E.W. C.J.F. is supported by a fellowship from Merck, Sharp & Dohme.
‡ The Pennsylvania State University.
§ Research Institute of Scripps Clinic.

[1] Abbreviations: COSY, correlated spectroscopy; 2D, two dimensional; DHFR, dihydrofolate reductase; DTT, dithiothreitol; H_2F, 7,8-dihydrofolate; H_4F, 5,6,7,8-tetrahydrofolate; MTX, methotrexate; NOE, nuclear Overhauser effect; NOESY, two-dimensional proton nuclear Overhauser spectroscopy; 2Q, two-quantum spectroscopy; 2QF-COSY, double quantum filtered COSY; ROESY, rotating frame Overhauser enhancement spectroscopy; TOCSY, total correlation spectroscopy.

0006-2960/90/0429-9667$02.50/0

mutants. In the present paper we report the assignment of residues near or at the active site based on site-specific mutagenesis of key residues and knowledge of the crystal structure. We have relied on the crystal structure for making assignments, rather than use the common backbone sequential assignment procedure (Billeter et al., 1982), because only ca. 60% of the expected of NH–$C^{\alpha}H$ cross peaks are observed in the COSY spectrum of DHFR in 90% ^1H_2O/10% ^2H_2O solution. A similar method has been used successfully to assign resonances of myoglobin, a protein of comparable size, on the basis of networks of NOE connectivities and the X-ray crystal structure (Dalvit & Wright, 1987).

Materials and Methods

Protein Purification and Preparation. All mutant and wild-type cells were grown in L-broth medium for about 8–12 h. Wild type and the T35S, L28F, and L54F mutants were grown in *E. coli* strain W71-18 containing the appropriate plasmid. The L54I mutant and the F31V mutants were grown in *E. coli* strain SF-32, which is deficient in chromosomal wild-type DHFR. All proteins were purified by using a methotrexate affinity resin followed by a DEAE-Sephacel column which removed remaining nucleotides (Baccanari et al., 1977). Active fractions were pooled and precipitated by bringing the enzyme solution to 90% ammonium sulfate saturation. The proteins were stored as a precipitate at 4 °C until use. Appropriate volumes of the precipitated proteins were spun down at 4000*g*. Generally, 20–30 mg of protein was used in each preparation. The supernatant was decanted off, and the protein was redissolved in ca. 3 mL of 50 mM phosphate buffer [pH 6.80, 1 mM EDTA and 1 mM dithiothreitol (DTT)] and dialyzed in this same buffer twice. The final dialysis was done in 10 mM phosphate (pH 6.85, 0.025 mM DTT) over argon. For ^2H_2O experiments, the proteins were lyophilized and then exchanged with ^2H_2O for 30 min and lyophilized again. This process was repeated at least one more time. Lyophilized proteins were dissolved in 0.35 mL of 99.96% ^2H_2O and 200 mM KCl, with the final volumes being brought to 0.40 mL. Folic acid (J. T. Baker), which was purified before use, was added in 1:1 to 1:4 molar excess from approximately 100 mM stock ^2H_2O solutions (200 mM KCl). Final protein concentrations were approximately 3–4 mM and were determined spectrophotometrically by using a molar extinction coefficient of 31 100 M^{-1} cm^{-1} at 280 nm (Fierke et al., 1987). The pH of the protein solutions was always 6.80 ± 0.03, and meter readings were not corrected for isotope effects.

Subcloning and Construction of Mutant Enzymes. The construction of the F31V, R44L, H45Q, and L54I mutants have been previously described (Chen et al., 1987, 1985; Perry et al., 1987; Murphy & Benkovic, 1989) and were used without further modification. The L28F and L54F mutants were constructed and purified by Dr. C. R. Wagner in our laboratory. For the T35S mutant, the *Bam*HI fragment containing the DHFR gene was subcloned into the pMac vector system (the generous gift of Dr. J. Andrews) which is based on a gapped duplex method (Kramer et al., 1984). The gapped strand, which possesses a different antibiotic resistance (chloramphenicol) than the single, wild-type strand (ampicillin), contained the mutagenic oligonucleotide after annealing, gap filling (20 nM T4 polymerase, provided by Dr. T. L. Capson in our laboratory), and ligation (T4 ligase, IBI Biochemicals). This reaction was done in T4 ligase buffer (IBI Biochemicals) at room temperature for 2 h with an excess of dNTP's. Gene 32 (provided by Dr. T. L. Capson) was added 15 min after initiation of polymerization to a final concentration of 100 μg/mL. This mixed population plasmid was used to transform a mismatch repair deficient (*Mut S*) *E. coli* strain (BMH71-18) so that linkage between the antibiotic resistance marker and the mutation was maintained. After DNA isolation and purification, this mixed population of strands were allowed to segregate by transforming into an su^- cell line (W71-18) which did not suppress amber codons present in the respective antibiotic coding regions of the vector. Mutants were selected for on chloramphenicol plates (20 μg/mL). In this case, removal of a *Dra*I site was conferred by the mutagenic oligonucleotide, so candidates were chosen on the basis of the *Dra*I restriction digest. This vector was also used for expression of the protein. The entire gene was sequenced by using either single-stranded DNA or denatured double-stranded DNA as templates for dideoxy sequencing (Sanger et al., 1977).

NMR Measurements. ^1H NMR spectra were recorded in 99.96% ^2H_2O, and 90% ^1H_2O and 10% ^2H_2O at 303 K with Bruker AM-500 and AM-600 spectrometers equipped with Aspect 3000 computers and digital phase shifting hardware. Time-proportional phase incrementation (Bodenhausen et al., 1980; Marion & Wüthrich, 1983) was used to achieve quadrature detection in the ω_1 dimension. The data were processed on an Aspect 3000 data station or with SUN 3/160C, micro VAX II, VAX 360, or CONVEX C240 computers using the FTNMR program of Dr. Dennis Hare. For all experiments, the carrier was placed on the solvent resonance, and typically between 460–512 t_1 experiments were collected, each containing 2048 complex data points, except for the NOESY, TOCSY, and CAMELSPIN (ROSEY) experiments, which contained 4096 complex points per experiment. Generally, 64 transients were acquired per increment for 2QF-COSY experiments, whereas for NOESY, TOCSY, and ROESY experiments, 96 transients were acquired for each experiment. The total experimental time was between 15 and 24 h. The number of time domain points used in the transform and the phase shift of the sine bell window function depended on whether high-resolution or high-sensitivity spectra were desired.

The pulse sequences and phase cycling routines for 2QF-COSY (Rance et al., 1983) and 2Q experiments (Braunschweiler et al., 1983; Rance & Wright, 1986) were standard. Pure absorption Hahn–echo NOESY spectra (Bodenhausen et al., 1984; Davis, 1989) were collected with mixing times of 50, 100, and 200 ms. No evidence for spin diffusion could be detected in any of the NOESY spectra. The analysis of the NOE connectivities was done by using 100-ms NOESY spectra. TOCSY spectra were obtained by using WALTZ-16 mixing by the method of Rance (1987) with mixing times of 63 or 75 ms. A single ROSEY experiment (Bothner-By et al., 1984) was collected with a mixing time of 50 ms, with spin locking achieved by means of a pulse whose field strength was 2.8 kHz. For cosine modulated data, the first free induction decay was divided by 2 to suppress t_1 ridges (Otting et al., 1986). All spectra were processed and plotted in phase-sensitive mode and were referenced to the $^2H^1HO$ line at 4.73 ppm.

Results

Assignment Strategy. The initial step in making sequence-specific assignments for DHFR is the identification of side-chain spin systems. In particular, aromatic and methyl-containing amino acids were examined most closely due to their relative ease of identification in a protein of this size and, more importantly, due to our desire to assign key hydrophobic residues which play important roles in binding and catalysis. To accomplish this, we relied upon 2QF-COSY and 2Q experiments. In a protein of this molecular weight

(18 000), overlap of cross peaks and chemical shift degeneracy are common, so 2Q spectra were often useful in delineating scalar connectivities for side chains. TOCSY spectra were also useful, for example, in distinguishing between the aromatic spin systems of phenylalanines and tryptophans; DHFR from *E. coli* has 6 phenylalanines and 5 tryptophans. Additionally, analysis of 2QF-COSY, 2Q, and TOCSY spectra of site-directed mutants helped greatly in spin system *identification* because the mutations frequently result in minor spectral perturbations that remove spectral overlap or chemical shift degeneracy present in spectra of wild-type DHFR.

Sequence-specific assignments were made on the basis of cross peaks observed in the NOESY spectra and the interproton distances in the crystal structure of *E. coli* DHFR. Assignments were not made unless a network of NOE connectivities was found that corresponds to a unique set of amino acid residues in the crystal structure. Several site-directed mutants were used to make particular assignments, especially in the active site. Use of mutants was particularly important in cases where NOEs could not be interpreted unambiguously from the X-ray structure or where extensive networks of NOE connectivities were not available. Assignments of residues adjacent to the site of mutation follow easily from NOE connectivities to the mutated amino acid. Owing to possible conformational differences between the folate and MTX complexes, the latter being used in the crystal structure, active site mutants were also utilized to ensure unambiguous resonance assignments. The MTX–DHFR complex also exhibits multiple conformations which preclude the extensive assignments possible with the folate complex (Falzone, Benkovic, and Wright, unpublished results).

The assignments of the ring protons for tyrosine, phenylalanine, and histidine were based on unique interresidue NOEs. Comparison to the X-ray structure allowed specific assignments to be made for these aromatic protons. For example, the $C^{\delta}H$ and $C^{\epsilon}H$ of Tyr-128 can be discriminated because of a unique NOE from the $C^{\delta}H$ of Trp-133 to the $C^{\epsilon}H$ of Tyr-128. In the case of tryptophans, assignment of the ring protons was achieved by observing the NOE between the $N^{\epsilon}H$ and $C^{\zeta 2}H$ in 90% H_2O/10% ^2H_2O solutions. The $N^{\epsilon}H$ proton was assigned by its strong NOE to the $C^{\delta}H$ or by detecting cross peaks in the 2QF-COSY or TOCSY spectra in 90% H_2O/10% ^2H_2O solutions. The remaining protons of the tryptophan ring are easily assigned once the $C^{\zeta 2}H$ proton assignment is made.

Trp-30, Tyr-111, Phe-137, Phe-153, His-141, and Ile-155. DHFR contains a β-sheet consisting of 7 parallel strands and 1 antiparallel strand. By use of the nomenclature from the X-ray crystal structure (Bolin et al., 1982), there is a unique cluster of aromatic residues (Tyr-111, Phe-137, Phe-153, His-141, and Tyr-151) present in the βG, βH (the antiparallel strand), and βF strands. Additionally, Trp-30, located in the αB helix and pointing away from the dihydrofolate binding pocket, is positioned between Phe-137, Phe-153, and Tyr-111. Ile-155 is at the center of these four aromatic residues (Figure 1).

On the basis of the crystal structure, NOEs are expected between ring protons of Trp-30 and Tyr-111, Trp-30 and Phe-137, and Phe-137 and Phe-153. Ile-155 is at the center of this aromatic cluster, and at the surface of the protein, His-141 is close to Phe-153. NOEs to this histidine will help distinguish Phe-153 from Phe-137.

Assignments for the residues in this aromatic cluster were made on the basis of NOE connectivities. NOEs are observed from the $C^{\delta}H$ of a tyrosine ($C^{\delta}H$, 6.79 ppm; $C^{\epsilon}H$, 6.58 ppm)

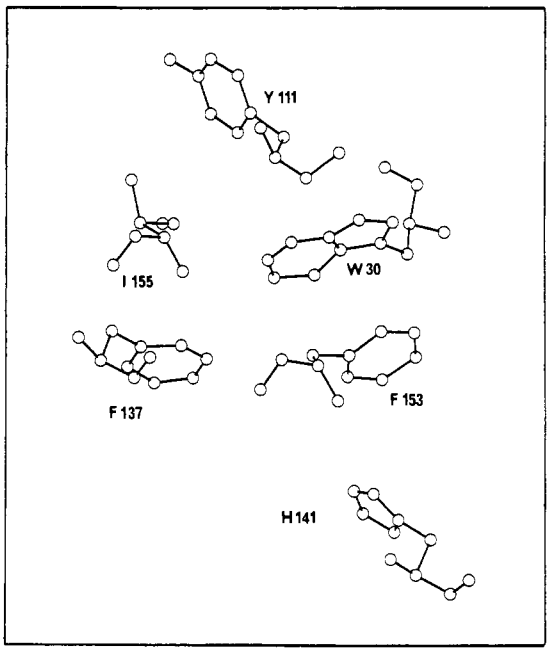

FIGURE 1: Spatial arrangement of the side chains Trp-30, Tyr-111, Phe-137, His-141, Phe-153, and Ile-155 from the X-ray crystal structure of DHFR (Bolin et al., 1982).

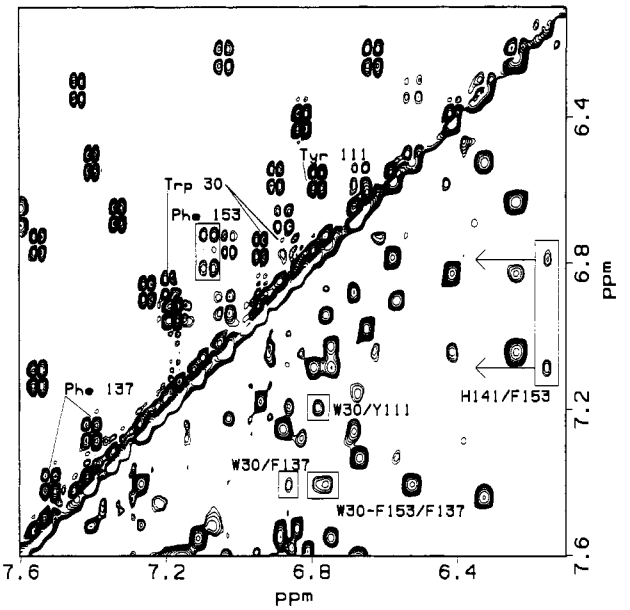

FIGURE 2: Region of a 2QF-COSY spectrum showing the assignments for Trp-30, Tyr-111, Phe-137, and Phe-153 is plotted above the diagonal. The corresponding region of a NOESY spectrum (100 ms) showing the NOEs between Trp-30 and Tyr-111, Trp-30 and Phe-137, Trp-30 and Phe-153, and His-141 and Phe-153 is plotted below the diagonal.

to the ring proton ($C^{\zeta 2}H$: 7.19 ppm) of a Trp spin system. This could occur at two locations in the DHFR molecule: Trp-30 to Tyr-111 and Trp-133 to Tyr-128. The latter assignment is less likely because all distances from the $C^{\delta}H$ and $C^{\epsilon}H$ protons of Tyr-128 to the benzenoid ring protons of Trp-133 are greater than 5 Å. In ^2H_2O, the $C^{\delta}H$ of Trp-133 is the only ring proton close enough for an observable NOE to Tyr-128 (see below). Nonetheless, we considered both assignments possible and searched for evidence that other aromatics were involved. A phenylalanine with chemical shift at 7.27 ($C^{\delta}H$), 7.41 ($C^{\epsilon}H$), and 7.52 ppm ($C^{\zeta}H$) was found to have NOEs to another phenylalanine ($C^{\delta}H$, 6.79 ppm; $C^{\epsilon}H$, 7.09 ppm; $C^{\zeta}H$, 6.75 ppm) and to the aforementioned tryp-

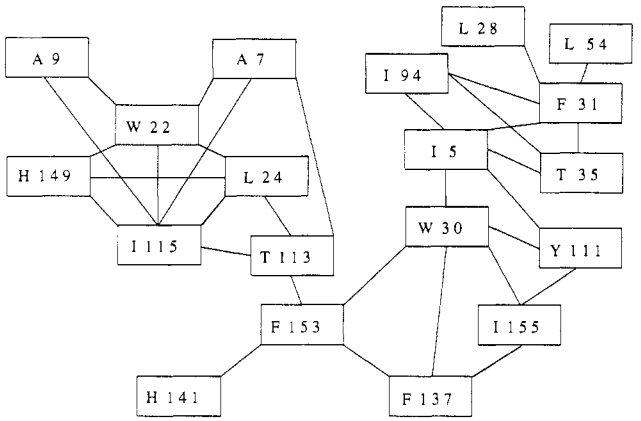

FIGURE 3: Schematic representation of the observed NOE connectivities for two hydrophobic clusters and some of the residues in the active site. Assignments originate at the site of mutated amino acids, and NOE connectivities are then followed to assign adjacent residues.

tophan (see Figure 2). The observation of this extended network of NOEs, involving two Phe, 1 Trp, and 1 Tyr residues, allows specific assignments to be made for Trp-30 and Tyr-111; to discriminate between Phe-137 and Phe-153, additional NOEs are required to the neighboring histidine. We have identified the imidazole ring proton resonances of all five histidines in DHFR. From the X-ray crystal structure, there is only one case (His-141 and Phe-153) where ring protons of His and Phe residues are within 5 Å. NOEs are observed between the $C^{\delta}H$ proton of a His ($C^{\delta}H$, 6.15, and $C^{\epsilon}H$, 8.45 ppm) and the $C^{\delta}H$ (6.79 ppm) and the $C^{\epsilon}H$ (7.09 ppm) protons of one of the two phenylalanines in the four aromatic ring cluster discussed above (Figure 2), thus allowing assignment of His-141 and Phe-153. The remaining Phe spin system is then assigned to Phe-137, completing the assignments of the aromatic amino acid side chains in this hydrophobic cluster. The NOE connectivities between these aromatic residues are summarized in Figure 3. Table I summarizes the chemical shifts for assigned side-chain resonances. Table II lists the observed NOEs between the assigned residues.

Ile-155, which resides in the center of this aromatic cluster (Figure 1), has its $C^{\delta}H_3$ resonance assigned on the basis of NOEs from Trp-30 ($C^{\eta}H$, $C^{\zeta 2}H$), Tyr-111 ($C^{\delta}H$, $C^{\epsilon}H$), and Phe-137 ($C^{\delta}H$, $C^{\epsilon}H$). The $C^{\gamma}H_3$ of Ile-155 is observed to have NOEs to $C^{\eta}H$ of Trp-30, to the ring protons of Tyr-111, and to the $C^{\delta}H$ protons of Phe-137 as well as intraresidue NOEs to its $C^{\delta}H_3$. Figure 3 depicts the interresidue NOE connectivities for these assignments and some of the assignments discussed below.

Phe-31, Leu-28, Leu-54, Thr-35, Ile-94, and Ile-5. Phe-31 is located in the αB helix and is an important hydrophobic residue in the H_2F binding pocket because of its edge to face interactions with both the pterin ring and *p*-aminobenzoyl group. Assignments of the ring protons of this phenylalanine in the DHFR–folate complex were initially based on 2QF-COSY and 2Q spectra of the F31V mutant. The 2QF-COSY spectrum of the mutant clearly revealed the disappearance of two resonances at 6.92 and 7.04 ppm. The third resonance of this spin system is nearly degenerate with the resonance at 7.04 ppm and is not easily observed in wild-type 2QF-COSY spectra. All three phenylalanine aromatic proton resonances can be found in the 2QF-COSY spectrum of the L54I mutant and in the TOCSY spectrum of the T35S mutant. The F31V mutant also showed a new set of methyl cross peaks in the 2QF-COSY spectrum ($C^{\gamma}H_3$s, 0.98, 0.50 ppm; $C^{\beta}H$: 1.63 ppm) which, as we will show later, belong to Val-31.

The chemical shifts for the F31V mutant are very similar to those of the wild-type protein (generally within ±0.05 ppm) with one notable exception. In the NOESY spectrum of the wild-type DHFR–folate complex, the ring protons of Phe-31 show NOEs to a ring current shifted methyl resonance at 0.11 ppm. This methyl resonance is coupled to a proton at 3.46 ppm and is characteristic of a threonine or alanine spin system. However, in the F31V mutant, this methyl resonance is shifted downfield to 0.85 ppm with a concomitant shift of the coupled proton resonance to 3.98 ppm. These results are consistent with the removal, by mutagenesis, of the phenyl ring that is causing a ring current shift of this methyl group resonance. On the basis of crystal structure, this methyl group is likely to belong to Thr-35, and indeed ring current shift calculations [using the X-ray coordinates of the MTX complex of *E. coli*

Table I: Chemical Shifts (±0.01 ppm) of Assigned Residues in DHFR from *E. coli* (pH 6.8, T = 303 K)

	$C^{\delta}H$	$C^{\epsilon}H$	$C^{\zeta}H$
Phe-31	7.04	7.04	6.92
Phe-103	7.56	7.12	7.12
Phe-125	7.04	6.24	6.64
Phe-137	7.27	7.41	7.52
Phe-153	6.79	7.09	6.75
Tyr-111	6.79	6.58	
Tyr-128	6.83	6.41	

	$C^{\delta}H$	$N^{\epsilon}H$	$C^{\zeta 2}H$	$C^{\eta}H$	$C^{\zeta 3}H$	$C^{\epsilon 3}H$
Trp-22	6.98	10.39	7.26	6.88	6.68	
Trp-30	7.02	10.43	7.19	6.86	6.76	6.95
Trp-47	7.22	10.22	7.41	6.53	6.33	7.45
Trp-74	7.21	10.00	7.04	7.03	6.75	7.56
Trp-133	7.94	10.28	7.34	6.67	6.57	6.90

	$C^{\epsilon}H$	$C^{\delta}H$		$C^{\epsilon}H$	$C^{\delta}H$
His-45	8.20	7.31	His-141	8.45	6.15
His-114	7.65	6.65	His-149	7.77	7.42
His-124[a]	8.44	7.35			

	$C^{\alpha}H$	$C^{\beta}H_3$		$C^{\alpha}H$	$C^{\beta}H_3$
Ala-6	4.79	0.80	Ala-81	3.97	1.70
Ala-7	4.79	1.15	Ala-107	4.63	1.80
Ala-9	4.98	1.71			

	$C^{\gamma}H$	$C^{\delta}H_3$	$C^{\delta}H_3$
Leu-4	2.00	1.00	1.17
Leu-8	1.29	0.36	0.50
Leu-24	1.48	0.18	0.93
Leu-28	1.62	0.37	0.64
Leu-54	1.68	0.59	0.84
Leu-110	0.73	−0.79	0.59
Leu-112	1.12	−0.01	0.37
Leu-156	1.55	0.63	0.86

	$C^{\beta}H$	$C^{\gamma}H_3$	$C^{\gamma}H_3$
Val-72	1.30	−0.52	0.21
Val-75	2.25	0.66	0.76
Val-78	1.84	0.44	0.52
Val-93	2.29	0.20	0.72

	$C^{\beta}H$	$C^{\gamma}H_2$	$C^{\gamma}H_3$	$C^{\delta}H_3$
Ile-5	1.22	2.13, 2.20	1.04	0.35
Ile-61	0.86	−0.41, 0.04	0.27	−0.43
Ile-82	1.95	1.12, 2.12	0.93	0.96
Ile-94	2.69		0.92	
Ile-115	0.78	−0.13, 0.86	0.10	−0.82
Ile-155	1.68	0.99, 1.93	0.46	0.67

	$C^{\alpha}H$	$C^{\beta}H$	$C^{\gamma}H_3$
Ser-3	6.02	4.26	
Thr-35		3.46	0.11
Thr-73	4.39	3.81	1.12
Thr-113	5.10	3.92	0.76

	H7	H12/H16	H13/H15
folate	9.80	7.17	5.87

[a] Assignment of these resonances as $C^{\delta}H$ and $C^{\epsilon}H$ is by chemical shift and is not based on NOE information.

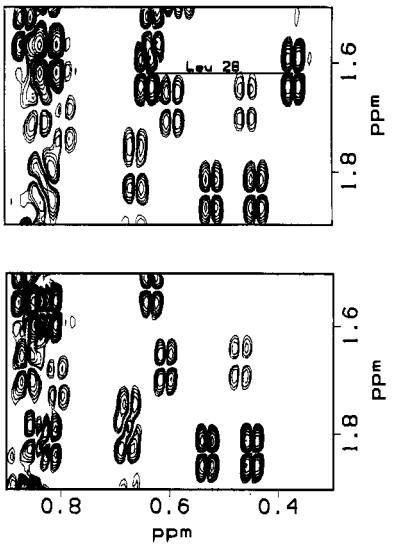

FIGURE 4: Regions of 2QF-COSY spectra of wild-type and L28F DHFR, with the assignment of Leu-28 indicated in the wild-type spectrum. These plots demonstrate how site-directed mutants may be used for assigning residues, particularly in the active site.

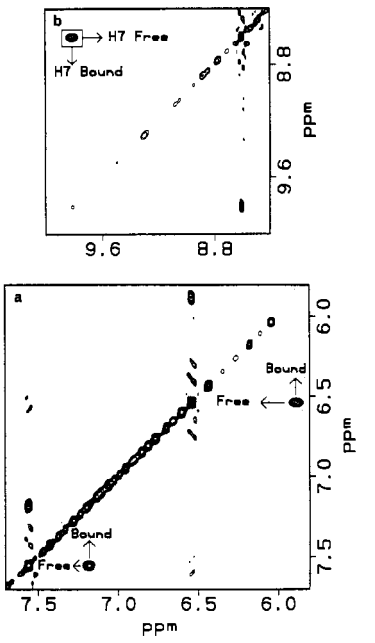

FIGURE 5: Positive levels of two regions of a 50-ms ROESY spectrum of a 4:1 folate–wild-type DHFR complex in ^2H_2O at 303 K. The free ligand resonances are easily distinguished from the protein resonances at these levels of folate. All ligand exchange rates are slow on the NMR time scale. (a) The cross peaks shown are from the slow exchange between the free and bound AA'BB' protons of the *p*-aminobenzoyl ring of folate. The resonances at 7.57 ppm (free) and 7.17 ppm (bound) are assigned as the H12/H16 protons (meta to N10). The resonances at 6.55 ppm (free) and 5.87 ppm (bound) are the H13/H15 protons and are ortho to N10 of folate. (b) An exchange cross peak between the free (8.61 ppm) and protein-bound H7 proton (9.80 ppm) on the pterin ring of folate.

DHFR (Bolin et al., 1982)] predict an upfield shift to 0.18 ppm for this resonance, based on the "random coil" shifts for the Thr $C^\gamma H_3$ group (Bundi & Wüthrich, 1979). These assignments were confirmed by constructing a mutant with serine at position 35. Comparison of the 2QF-COSY spectra of wild-type protein and T35S mutant shows the loss of the $C^\gamma H_3$–$C^\beta H$ cross peak attributed to Thr-35. In further support of the assignments, the NOEs from Phe-31 ring protons to 0.11 ppm are missing from the NOESY spectrum of the T35S mutant.

Leucine 28 also has an important hydrophobic interaction with the *p*-aminobenzoyl ring of bound H_2F. NOEs are observed between Phe-31 and leucine or valine methyl proton resonances at 0.37 and 0.64 ppm. Upon examination of the 2QF-COSY of the L28F mutant, these methyl cross peaks were found to disappear (Figure 4). Also, the NOEs observed between Phe-31 and the methyl resonances at 0.37 and 0.64 ppm for wild-type DHFR are absent from the NOESY spectrum of the L28F mutant, thus confirming the assignment. Finally, a new Phe spin system attributed to Phe-28 was observed in the 2QF-COSY spectrum of the L28F mutant ($C^\delta H$, $C^\epsilon H$, and $C^\zeta H$ at 6.86, 6.58, and 6.96 ppm, respectively).

Leu-54, which is positioned on the opposite side of the *p*-aminobenzoyl ring of bound folate from Leu-28, can also be assigned using site-directed mutagenesis. Cross peaks of a Leu/Val spin system ($C^\delta H_3$s, 0.59, 0.84 ppm; $C^\gamma H$, 1.68 ppm) are absent from the 2QF-COSY spectrum of the L54F and L54I mutants, and resonances of new Phe and Ile spin systems appear [$C^\delta H$, $C^\epsilon H$, and $C^\zeta H$ at 7.25, 6.87, and 6.15 ppm (Phe-54); $C^\delta H_3$, 0.74 ppm; $C^\gamma Hs$, 1.00, 1.60 ppm (Ile-54)]. The NOESY spectrum of wild-type DHFR showed that the Leu $C^\delta H_3$ resonance at 0.59 ppm had NOEs both to the *p*-aminobenzoyl AA'BB' ring of folate and to Phe-31. Thus, side-chain proton resonances of all of the residues which are important for binding the *p*-aminobenzoyl ring of H_2F can be assigned.

The protons of the *p*-aminobenzoyl ring system may be assigned by observing their slow exchange on the NMR time scale between free and bound resonances in a 50-ms ROESY experiment (Figure 5a). Discriminating between exchange cross peaks and rotating frame NOEs is possible in a 2D ROESY experiment due to the difference in sign of their cross peaks: exchange cross peaks have positive intensity relative to the diagonal while rotating frame NOEs are negative. The bound H7 resonance, which is in slow exchange (on the NMR time scale) with its free resonance, may also be assigned in this 2D ROESY experiment (Figure 5b) by observing its exchange cross peak.

An isolated Ile $C^\gamma H_3$–$C^\beta H$ cross peak ($C^\gamma H_3$, 0.92 ppm; $C^\beta H$, 2.69 ppm) is easily observed owing to a relatively strong downfield shift of the $C^\beta H$ (random coil, 1.90; observed, 2.69 ppm). The remaining protons of this spin system could not be identified although a cross peak from the $C^\beta H$ to a putative $C^\gamma H$ is observed at 1.04 ppm. However, this places one of the $C^\gamma H$–$C^\delta H_3$ cross peaks in an extremely crowded region and thus explains the inability to completely identify this side chain. This Ile γ-methyl showed NOEs to protons of two residues previously assigned with aid of site-directed mutants: Phe-31 ($C^\epsilon H$, $C^\zeta H$ protons) and $C^\gamma H_3$ of Thr-35. NOEs from Phe-31 and Thr-35 to an Ile $C^\gamma H_3$ are possible for only two residues: Ile-5 and Ile-94. The Ile-5 resonances are assigned below, so this $C^\gamma H_3$ is part of Ile-94. The $C^\beta H$ shows NOEs to Phe-31's $C^\epsilon H$ *and* to the bound H7 proton on the pterin ring of folate (see Figure 6). The existence of an NOE between H7 and Ile-94's $C^\beta H$ immediately places constraints on the orientation of the pterin ring: its conformation is similar to the conformation in a productive complex (Charlton et al., 1979). This is in contrast to the orientation of the pterin ring in the MTX complex, which from the X-ray crystal structure (Bolin et al., 1982) and our NMR experiments (Falzone, Benkovic, and Wright, unpublished results) is in an "upside-down" conformation, i.e., rotated ca. 180° about the C6–C9 bond. Also, under our conditions for the binary folate complex, we have not detected H7 in multiple environments; i.e., only a single bound H7 resonance is observed in both 1D (data not shown) and 2D ROSEY and NOESY experiments (Figure 5b).

Table II: List of Interresidue ^{1}H NOEs Observed in the Folate Complex of *E. coli* DHFR[a]

residue	proton	NOEs
Ser-3	$C^{\alpha}H$	$C^{\delta 1}H_3$, $C^{\delta 2}H_3$ Leu-4; $C^{\beta}H_3$ Ala-107; $C^{\delta 2}H_3$ Leu-110; $C^{\delta}H$, $C^{\epsilon}H$ Tyr-111
	$C^{\beta}H_2$	$C^{\delta}H$, $C^{\delta}H$ Tyr-111
Leu-4	$C^{\alpha}H$	$C^{\beta}H$, $C^{\gamma 1}H_3$, $C^{\gamma 2}H_3$ Val-93
	$C^{\beta}H_2$	$C^{\zeta}H$ Phe-125
	$C^{\gamma}H$	$C^{\gamma 1}H_3$ Val-93; $C^{\delta 2}H_3$ Leu-110
	$C^{\delta 1}H_3$	$C^{\alpha}H$ Ser-3; $C^{\gamma 1}H_3$, $C^{\gamma 2}H_3$ Val-93; $C^{\delta 2}H_3$ Leu-110; $C^{\epsilon}H$, $C^{\zeta}H$ Phe-125
	$C^{\delta 2}H_3$	$C^{\alpha}H$ Ser-3; $C^{\gamma 1}H_3$ Val-93; $C^{\delta 2}H_3$ Leu-110; $C^{\epsilon}H$, $C^{\zeta}H$ Phe-125
Ile-5	$C^{\alpha}H$	$C^{\delta 2}H_3$ Leu-112
	$C^{\beta}H$	$C^{\delta}H$ Tyr-111
	$C^{\gamma}H_3$	$C^{\delta}H$, $C^{\epsilon}H$, $C^{\zeta}H$ Phe-31; $C^{\gamma}H_3$ Thr-35; $C^{\alpha}H$ Ile-94; H7 folate
	$C^{\delta}H_3$	$N^{\epsilon}H$, $C^{\delta}H$ Trp-30; $C^{\delta}H$, $C^{\epsilon}H$ Phe-31; $C^{\delta}H$ Tyr-111
Ala-6	$C^{\beta}H_3$	$C^{\delta 1}H_3$, $C^{\delta 2}H_3$ Leu-8; $C^{\delta 1}H_3$ Leu-112; $C^{\delta}H$, $C^{\epsilon}H$, $C^{\zeta}H$ Phe-125
Ala-7	$C^{\alpha}H$	$C^{\beta}H$ Thr-113
	$C^{\beta}H_3$	$N^{\epsilon}H$, $C^{\zeta 2}H$ Trp-22; $C^{\beta}H$ Thr-113; $C^{\delta}H_3$ Ile-115
Leu-8	$C^{\delta 1}H_3$	$C^{\beta}H_3$ Ala-6; $C^{\delta 1}H_3$ Leu-112; $C^{\epsilon}H$ His-114; $C^{\delta}H$, $C^{\epsilon}H$ Phe-125; $C^{\epsilon}H$ Tyr-128
	$C^{\delta 2}H_3$	$C^{\beta}H_3$ Ala-6; $C^{\delta 1}H_3$ Leu-112; $C^{\epsilon}H$ His-114; $C^{\delta}H$, $C^{\epsilon}H$ Phe-125; $C^{\epsilon}H$ Tyr-128
Ala-9	$C^{\alpha}H$	$C^{\beta}H$, $C^{\delta}H_3$ Ile-115
	$C^{\beta}H_3$	$C^{\zeta 3}H$, $C^{\eta}H$ Trp-22; $C^{\gamma}H_3$ Ile-115
Trp-22	$N^{\epsilon}H$	$C^{\beta}H_3$ Ala-7; $C^{\delta 1}H_3$ Leu-24; $C^{\delta}H_3$ Ile-115
	$C^{\delta}H$	$C^{\gamma}H$, $C^{\delta 1}H_3$, $C^{\delta 2}H_3$ Leu-24; $C^{\gamma}H_3$, $C^{\delta}H_3$ Ile-115
	$C^{\zeta 3}H$	$C^{\beta}H_3$ Ala-9; $C^{\gamma}H_3$, $C^{\delta}H_3$ Ile-115; $C^{\epsilon}H$ His-149
	$C^{\eta}H$	$C^{\beta}H_3$ Ala-9; $C^{\delta}H_3$ Ile-115
	$C^{\zeta 2}H$	$C^{\beta}H_3$ Ala-7; $C^{\delta}H_3$ Ile-115
Leu-24	$C^{\gamma}H$	$C^{\delta}H$ Trp-22
	$C^{\delta 1}H_3$	$N^{\epsilon}H$, $C^{\delta}H$ Trp-22; $C^{\gamma}H_3$ Thr-113; $C^{\gamma 1}H$, $C^{\delta}H_3$ Ile-115; $C^{\epsilon}H$ His-149
	$C^{\delta 2}H_3$	$C^{\delta}H$ Trp-22
Leu-28	$C^{\delta 1}H_3$	$C^{\delta}H$ Phe-31; H12, H16 folate
	$C^{\delta 2}H_3$	$C^{\delta}H$, $C^{\epsilon}H$ Phe-31; assigned by mutation (L28F mutant)
Trp-30	$N^{\epsilon}H$	$C^{\delta}H_3$ Ile-5; $C^{\delta}H$ Phe-153
	$C^{\delta}H$	$C^{\delta}H_3$ Ile-5
	$C^{\zeta 3}H$	$C^{\epsilon}H$ Phe-137
	$C^{\eta}H$	$C^{\gamma}H_3$, $C^{\delta}H_3$ Ile-155; $C^{\epsilon}H$ Phe-137
	$C^{\zeta 2}H$	$C^{\delta}H$ Tyr-111; $C^{\delta}H_3$ Ile-155
Phe-31	$C^{\delta}H$	$C^{\gamma}H_3$, $C^{\delta}H_3$ Ile-5; $C^{\delta 1}H_3$, $C^{\delta 2}H_3$ Leu-28; $C^{\gamma}H_3$ Thr-35
	$C^{\epsilon}H$	$C^{\gamma}H_3$, $C^{\delta}H_3$ Ile-5; $C^{\gamma}H_3$ Thr-35; $C^{\delta 2}H_3$ Leu-28; $C^{\delta 1}H_3$, $C^{\delta 2}H_3$ Leu-54; $C^{\alpha}H$, $C^{\beta}H$, $C^{\gamma}H_3$ Ile-94; H12, H16 folate
	$C^{\zeta}H$	$C^{\gamma}H_3$ Ile-5; $C^{\gamma}H_3$ Thr-35; $C^{\delta 2}H_3$ Leu-54; $C^{\gamma}H_3$ Ile-94; also assigned by F31V mutant
Thr-35	$C^{\gamma}H_3$	$C^{\gamma}H_3$ Ile-5; $C^{\delta}H$, $C^{\epsilon}H$, $C^{\zeta}H$ Phe-31; $C^{\gamma}H_3$ Ile-94; also assigned by T35S mutant
His-45	$C^{\delta}H$	$C^{\gamma 1}H_3$ Leu-44 (R44L mutant)
	$C^{\epsilon}H$	$C^{\gamma 1}H_3$ Leu-44 (R44L mutant); assigned by H45Q mutant
Trp-47	$N^{\epsilon}H$	$C^{\zeta 2}H$, $C^{\eta}H$ Trp-74
	$C^{\delta}H$	$C^{\gamma}H_3$, $C^{\delta}H_3$ Ile-61; $C^{\eta}H$ Trp-74
	$C^{\epsilon 3}H$	$C^{\gamma}H_3$, $C^{\delta}H_3$ Ile-61; $C^{\gamma 2}H_3$ Val-72
	$C^{\zeta 3}H$	$C^{\delta}H_3$ Ile-61; $C^{\gamma 1}H$, $C^{\gamma 2}H_3$ Val-72
	$C^{\eta}H$	$C^{\gamma 1}H_3$, $C^{\gamma 2}H_3$ Val-72
	$C^{\zeta 2}H$	$C^{\gamma 1}H_3$, $C^{\gamma 2}H_3$ Val-72; $C^{\zeta 2}H$ Trp-74
Leu-54	$C^{\delta 1}H_3$	$C^{\epsilon}H$ Phe-31; H12, H16 folate
	$C^{\delta 2}H_3$	$C^{\epsilon}H$, $C^{\zeta}H$ Phe-31; assigned by L54F mutation
Ile-61	$C^{\gamma 1}H$	$C^{\gamma 1}H_3$ Val-72
	$C^{\gamma}H_3$	$C^{\delta}H$, $C^{\epsilon 3}H$ Trp-47; $C^{\epsilon 3}H$, $C^{\zeta 3}H$, $C^{\eta}H$ Trp-74
	$C^{\delta}H_3$	$C^{\delta}H$, $C^{\epsilon 3}H$, $C^{\zeta 3}H$ Trp-47; $C^{\beta}H$, $C^{\gamma 1}H_3$, $C^{\gamma 2}H_3$ Val-72; $C^{\epsilon 3}H$, $C^{\zeta 3}H$, $C^{\eta}H$ Trp-74
Val-72	$C^{\beta}H$	$C^{\delta}H_3$ Ile-61
	$C^{\gamma 1}H_3$	$C^{\zeta 3}H$, $C^{\eta}H$, $C^{\zeta 2}H$ Trp-47; $C^{\gamma 1}H$, $C^{\delta}H_3$ Ile-61; $N^{\epsilon}H$, $C^{\delta}H$, $C^{\zeta 2}H$ Trp-74
	$C^{\gamma 2}H_3$	$C^{\epsilon 3}H$, $C^{\zeta 3}H$, $C^{\eta}H$, $C^{\zeta 2}H$ Trp-47; $C^{\delta}H_3$ Ile-61; $C^{\epsilon 3}H$ Trp-74
Thr-73	$C^{\alpha}H$	$C^{\delta}H$ Trp-74
	$C^{\beta}H$	$C^{\gamma 1}H_3$ Val-75
	$C^{\gamma}H_3$	$C^{\gamma 1}H_3$, $C^{\gamma 2}H_3$ Val-75
Trp-74	$N^{\epsilon}H$	$C^{\gamma 1}H_3$ Val-72
	$C^{\delta}H$	$C^{\gamma 1}H_3$ Val-72; $C^{\alpha}H$ Thr-73
	$C^{\epsilon 3}H$	$C^{\gamma}H_3$, $C^{\delta}H_3$ Ile-61; $C^{\gamma 2}H_3$ Val-72
	$C^{\zeta 3}H$	$C^{\gamma}H_3$, $C^{\delta}H_3$ Ile-61
	$C^{\eta}H$	$N^{\epsilon}H$, $C^{\delta}H$ Trp-47; $C^{\gamma}H_3$, $C^{\delta}H_3$ Ile-61
	$C^{\zeta 2}H$	$N^{\epsilon}H$, $C^{\zeta 2}H$ Trp-47; $C^{\gamma 1}H_3$ Val-72
Val-75	$C^{\gamma 1}H_3$	$C^{\beta}H$, $C^{\gamma}H_3$ Thr-73; $C^{\alpha}H$, $C^{\beta}H_3$ Ala-81
	$C^{\gamma 2}H_3$	$C^{\gamma}H_3$ Thr-73; $C^{\alpha}H$, $C^{\beta}H_3$ Ala-81
Val-78	$C^{\alpha}H$	$C^{\beta}H_3$ Ala-81; $C^{\epsilon}H$ Phe-103
	$C^{\gamma 1}H_3$	$C^{\delta}H_3$ Ile-82; $C^{\delta}H$, $C^{\epsilon}H$ Phe-103
	$C^{\gamma 2}H_3$	$C^{\delta}H$, $C^{\epsilon}H$ Phe-103
Ala-81	$C^{\alpha}H$	$C^{\gamma 1}H_3$, $C^{\gamma 2}H_3$ Val-75
	$C^{\beta}H_3$	$C^{\gamma 1}H_3$, $C^{\gamma 2}H_3$ Val-75; $C^{\alpha}H$ Val-78; $C^{\epsilon}H$ Phe-103
Ile-82	$C^{\gamma 1}H$	$C^{\epsilon}H$ Phe-103
	$C^{\gamma 2}H$	$C^{\epsilon}H$ Phe-103
	$C^{\delta}H_3$	$C^{\gamma 1}H_3$ Val-78; $C^{\delta}H$, $C^{\epsilon}H$ Phe-103
Val-93	$C^{\beta}H$	$C^{\alpha}H$ Leu-4
	$C^{\gamma 1}H_3$	$C^{\alpha}H$, $C^{\gamma}H$, $C^{\delta 1}H_3$, $C^{\delta 2}H_3$ Leu-4; $C^{\delta}H$, $C^{\epsilon}H$ Phe-103
	$C^{\gamma 2}H_3$	$C^{\alpha}H$, $C^{\delta 2}H_3$ Leu-4; $C^{\delta}H$ Phe-103
Ile-94	$C^{\alpha}H$	$C^{\gamma}H_3$ Ile-5; $C^{\epsilon}H$ Phe-31
	$C^{\beta}H$	$C^{\epsilon}H$ Phe-31; H7 folate
	$C^{\gamma}H_3$	$C^{\delta}H$, $C^{\zeta}H$ Phe-31; $C^{\gamma}H_3$ Thr-35
Phe-103	$C^{\delta}H$	$C^{\gamma 1}H_3$, $C^{\gamma 2}H_3$ Val-78; $C^{\delta}H_3$ Ile-82; $C^{\gamma 1}H_3$, $C^{\gamma 2}H_3$ Val-93
	$C^{\epsilon}H$	$C^{\alpha}H$, $C^{\gamma 1}H_3$, $C^{\gamma 2}H_3$ Val-78; $C^{\beta}H_3$ Ala-81; $C^{\gamma 1}H$, $C^{\gamma 2}H$, $C^{\delta}H_3$ Ile-82; $C^{\gamma 1}H_3$ Val-93
Ala-107	$C^{\beta}H_3$	$C^{\alpha}H$ Ser-3; $C^{\delta 2}H_3$ Leu-110; $C^{\zeta 3}H$, $C^{\eta}H$ Trp-133

Table II (Continued)

residue	proton	NOEs
Leu-110	$C^{\delta 1}H_3$	$C^{\delta 1}H_3$, $C^{\delta 2}H_3$ Leu-112; $C^{\epsilon}H$, $C^{\zeta}H$ Phe-125; $C^{\delta}H$, $C^{\epsilon}H$ Tyr-128; $C^{\epsilon 3}H$, $C^{\zeta 3}H$, $C^{\eta}H$, $C^{\zeta 2}H$ Trp-133; $C^{\delta 1}H_3$ Leu-156
	$C^{\delta 2}H_3$	$C^{\alpha}H$ Ser-3; $C^{\gamma}H$, $C^{\delta 1}H_3$, $C^{\delta 2}H_3$ Leu-4; $C^{\beta}H_3$ Ala-107; $C^{\epsilon}H$, $C^{\zeta}H$ Phe-125; $C^{\zeta 3}H$, $C^{\eta}H$ Trp-133
Tyr-111	$C^{\delta}H$	$C^{\alpha}H$, $C^{\beta}H_2$ Ser-3; $C^{\beta}H$, $C^{\delta}H_3$ Ile-5; $C^{\zeta 2}H$ Trp-30; $C^{\gamma}H_3$, $C^{\delta}H_3$ Ile-155
	$C^{\epsilon}H$	$C^{\alpha}H$, $C^{\beta}H_2$ Ser-3; $C^{\gamma}H_3$, $C^{\delta}H_3$ Ile-155
Leu-112	$C^{\delta 1}H_3$	$C^{\beta}H_3$ Ala-6; $C^{\delta 1}H_3$, $C^{\delta 2}H_3$ Leu-8; $C^{\delta 1}H_3$ Leu-110; $C^{\epsilon}H$ His-114; $C^{\delta}H$, $C^{\epsilon}H$, $C^{\zeta}H$ Phe-125; $C^{\delta}H$, $C^{\epsilon}H$ Tyr-128;
	$C^{\delta 2}H_3$	$C^{\alpha}H$ Ile-5; $C^{\delta 1}H_3$ Leu-110; $C^{\delta}H$, $C^{\epsilon}H$ His-114; $C^{\delta}H$, $C^{\epsilon}H$ Tyr-128
Thr-113	$C^{\beta}H$	$C^{\alpha}H$, $C^{\beta}H_3$ Ala-7
	$C^{\gamma}H_3$	$C^{\delta 1}H_3$ Leu-24; $C^{\gamma 1}H$, $C^{\delta}H_3$ Ile-115; $C^{\delta}H$, $C^{\epsilon}H$, $C^{\zeta}H$ Phe-153
His-114	$C^{\delta}H$	$C^{\delta 2}H_3$ Leu-112
	$C^{\epsilon}H$	$C^{\delta 1}H_3$, $C^{\delta 2}H_3$ Leu-8; $C^{\delta 1}H_3$, $C^{\delta 2}H_3$ Leu-112; $C^{\epsilon}H$ Tyr-128; $C^{\delta 1}H_3$ Leu-156
Ile-115	$C^{\beta}H$	$C^{\alpha}H$ Ala-9
	$C^{\gamma 1}H$	$C^{\delta 1}H_3$ Leu-24; $C^{\gamma}H_3$ Thr-113
	$C^{\gamma}H_3$	$C^{\beta}H_3$ Ala-9; $C^{\delta}H$, $C^{\zeta 3}H$ Trp-22; $C^{\delta}H$ His-149
	$C^{\delta}H_3$	$C^{\beta}H_3$ Ala-7; $C^{\alpha}H$ Ala-9; $N^{\epsilon}H$, $C^{\delta}H$, $C^{\zeta 3}H$, $C^{\eta}H$, $C^{\zeta 2}H$ Trp-22; $C^{\delta 1}H_3$ Leu-24; $C^{\gamma}H_3$ Thr-113
Phe-125	$C^{\delta}H$	$C^{\beta}H_3$ Ala-6; $C^{\delta 1}H_3$, $C^{\delta 2}H_3$ Leu-8; $C^{\delta 1}H_3$ Leu-112; $C^{\delta}H$, $C^{\epsilon}H$ Tyr-128
	$C^{\epsilon}H$	$C^{\delta 1}H_3$, $C^{\delta 2}H_3$ Leu-4; $C^{\beta}H_3$ Ala-6; $C^{\delta 1}H_3$, $C^{\delta 2}H_3$ Leu-8; $C^{\delta 1}H_3$, $C^{\delta 2}H_3$ Leu-110; $C^{\delta 1}H_3$ Leu-112; $C^{\delta}H$, $C^{\epsilon}H$ Tyr-128
	$C^{\zeta}H$	$C^{\beta}H_2$, $C^{\delta 1}H_3$, $C^{\delta 2}H_3$ Leu-4; $C^{\beta}H_3$ Ala-6; $C^{\delta 1}H_3$, $C^{\delta 2}H_3$ Leu-110; $C^{\delta 1}H_3$ Leu-112;
Tyr-128	$C^{\delta}H$	$C^{\delta 1}H_3$ Leu-110; $C^{\delta 1}H_3$, $C^{\delta 2}H_3$ Leu-112; $C^{\delta}H$, $C^{\epsilon}H$ Phe-125; $N^{\epsilon}H$, $C^{\delta}H$ Trp-133; $C^{\delta 1}H_3$, $C^{\delta 2}H_3$ Leu-156
	$C^{\epsilon}H$	$C^{\delta 1}H_3$, $C^{\delta 2}H_3$ Leu-8; $C^{\delta 1}H_3$ Leu-110; $C^{\delta 1}H_3$, $C^{\delta 2}H_3$ Leu-112; $C^{\epsilon}H$ His-114; $C^{\delta}H$, $C^{\epsilon}H$ Phe-125; $C^{\delta}H$ Trp-133; $C^{\delta 1}H_3$, $C^{\delta 2}H_3$ Leu-156
Trp-133	$N^{\epsilon}H$	$C^{\delta}H$ Tyr-128
	$C^{\delta}H$	$C^{\delta}H$, $C^{\epsilon}H$ Tyr-128; $C^{\delta 2}H_3$ Leu-156
	$C^{\epsilon 3}H$	$C^{\delta 1}H_3$ Leu-110;
	$C^{\zeta 3}H$	$C^{\beta}H_3$ Ala-107; $C^{\delta 1}H_3$, $C^{\delta 2}H_3$ Leu-110
	$C^{\eta}H$	$C^{\beta}H_3$ Ala-107; $C^{\delta 1}H_3$, $C^{\delta 2}H_3$ Leu-110
	$C^{\zeta 2}H$	$C^{\delta 1}H_3$ Leu-110
Phe-137	$C^{\delta}H$	$C^{\gamma}H_3$, $C^{\delta}H_3$ Ile-155
	$C^{\epsilon}H$	$C^{\zeta 3}H$, $C^{\eta}H$ Trp-30; $C^{\delta}H$ Phe-153; $C^{\delta}H_3$ Ile-155
	$C^{\zeta}H$	$C^{\delta}H$ Phe-153
His-141	$C^{\delta}H$	$C^{\delta}H$, $C^{\epsilon}H$ Phe-153
His-149	$C^{\delta}H$	$C^{\gamma}H_3$ Ile-115
	$C^{\epsilon}H$	$C^{\zeta 3}H$ Trp-22; $C^{\delta 1}H_3$ Leu-24
Phe-153	$C^{\delta}H$	$N^{\epsilon}H$ Trp-30; $C^{\gamma}H_3$ Thr-113; $C^{\epsilon}H$, $C^{\zeta}H$ Phe-137; $C^{\delta}H$ His-141
	$C^{\epsilon}H$	$C^{\gamma}H_3$ Thr-113; $C^{\delta}H$ His-141
	$C^{\zeta}H$	$C^{\gamma}H_3$ Thr-113
Ile-155	$C^{\gamma}H_3$	$C^{\eta}H$ Trp-30; $C^{\delta}H$, $C^{\epsilon}H$ Tyr-111; $C^{\delta}H$ Phe-137
	$C^{\delta}H_3$	$C^{\eta}H$, $C^{\zeta 2}H$ Trp-30; $C^{\delta}H$, $C^{\epsilon}H$ Tyr-111; $C^{\delta}H$, $C^{\epsilon}H$ Phe-137
Leu-156	$C^{\delta 1}H_3$	$C^{\delta 1}H_3$ Leu-110; $C^{\epsilon}H$ His-114; $C^{\delta}H$, $C^{\epsilon}H$ Tyr-128
	$C^{\delta 2}H_3$	$C^{\delta}H$, $C^{\epsilon}H$ Tyr-128; $C^{\delta}H$ Trp-133
folate	H7	$C^{\gamma}H_3$ Ile-5; $C^{\beta}H$ Ile-94
	H12, 16	$C^{\delta 1}H_3$ Leu-28; $C^{\epsilon}H$ Phe-31; $C^{\delta 1}H_3$ Leu-54

[a] The superscript numbers on Leu or Val methyls or Ile $C^{\gamma}H$ refer to their relative chemical shift (1 = high field, 2 = low field methyl).

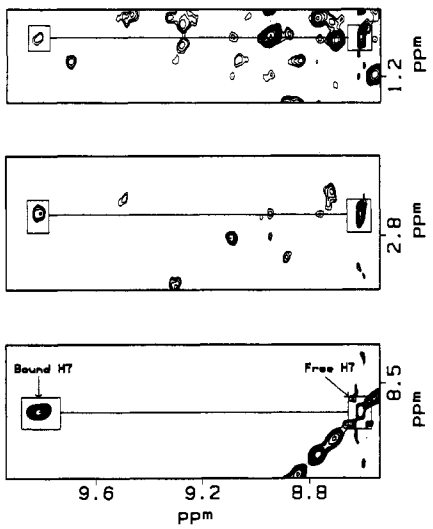

FIGURE 6: Regions of a 100-ms NOESY spectrum of a 4:1 folate–wild-type DHFR complex showing the exchange cross peak between free (8.61 ppm) and bound H7 (9.80 ppm) of folate in the bottom panel. The middle panel shows the direct NOE from bound H7 and the transferred NOE from free H7 to the $C^{\beta}H$ of Ile-94. The top panel shows the direct NOE and the transferred NOE between H7 and the $C^{\gamma}H_3$ of Ile-5.

Ile-5 $C^{\delta}H_3$ is positioned between the $C^{\delta}H$ of Trp-30, the aromatic ring of Tyr-111, and the aromatic ring of Phe-31. NOEs from a $C^{\delta}H_3$ of an Ile spin system at 0.35 ppm are observed to the $N^{\epsilon}H$ and $C^{\delta}H$ of Trp-30, the $C^{\beta}H$ of Tyr-111, and the $C^{\delta}H$ and $C^{\epsilon}H$ of Phe-31. With this unique complement of NOEs, this $C^{\delta}H_3$ is assigned as Ile-5. Additionally, a $C^{\gamma}H_3$ at 1.04 ppm is found to have NOEs to Phe-31 ($C^{\epsilon}H$, $C^{\zeta}H$), Thr-35 ($C^{\gamma}H_3$), and $C^{\alpha}H$ of Ile-94; it also has intraresidue NOEs to the $C^{\delta}H_3$ at 0.35 ppm. With the other Ile $C^{\gamma}H_3$ within 5 Å of Trp-30, Phe-31, and Tyr-111 having been assigned, we assign this methyl group as part of Ile-5. It is important to note that when transformed under high-sensitivity conditions, H7 of folate is observed to have an NOE to this $C^{\gamma}H_3$ (Figure 6). This NOE, which is not unexpected given that the $C^{\gamma}H_3$ of Ile-5 and $C^{\beta}H$ of Ile-94 are within 3.2 Å of each other, is also consistent with binding of the pterin ring in a non-MTX-like conformation.

Trp-47, Trp-74, Ile-61, and Val-72. Trp-47 resides in the αC helix with its ring making hydrophobic contact with the ring of Trp-74 in the βD strand; the side chains are oriented such that the five-membered ring of Trp-47 is over the benzenoid ring of Trp-74. Both Ile-61 and Val-72 are positioned below these rings, with the Val-72 methyl groups slightly closer to Trp-47 benzenoid ring and close to the $C^{\delta}H$ of Trp-74. The Ile $C^{\gamma}H_3$ group is near the benzenoid ring of Trp-74, and the Ile $C^{\delta}H_3$ is close to the $C^{\delta}H$ of Trp-47 (Figure 7).

A $C^{\delta}H$ of a Trp (7.22 ppm) is observed to have an NOE to a proton ($C^{\eta}H$, 7.03 ppm) of another Trp spin system. This latter Trp spin system, though not easily identified in the 2QF-COSY spectra due to the near degeneracy of two of its protons ($C^{\zeta 2}H$, 7.04 ppm; $C^{\eta}H$, 7.03 ppm), can be finally assigned in a TOCSY spectrum of wild-type DHFR. NOEs between two tryptophans are only possible between Trp-47 and Trp-74. Furthermore, the observed $C^{\delta}H$ to $C^{\eta}H$ NOE suggests that the $C^{\delta}H$ is part of the Trp-47 spin system and that the

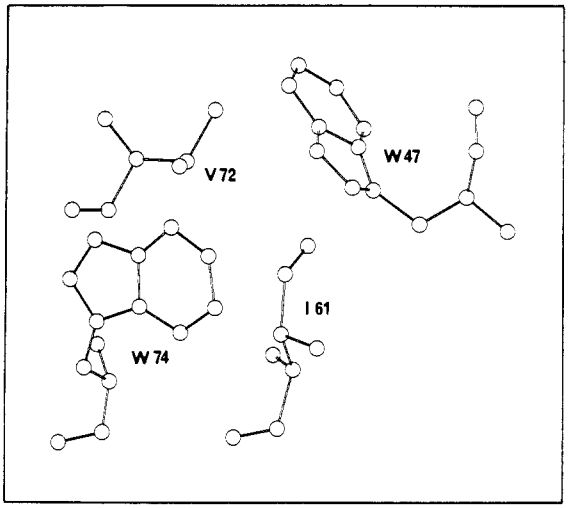

FIGURE 7: Orientation of the side chains Trp-47, Ile-61, Val-72, and Trp-74 in the X-ray crystal structure (Bolin et al., 1982). Note that the $C^{\delta}H$ of Trp-47 should have NOEs to the $C^{\delta}H_3$ of Ile-61 and the $C^{\gamma}H$ of Trp-74 (see Figure 8).

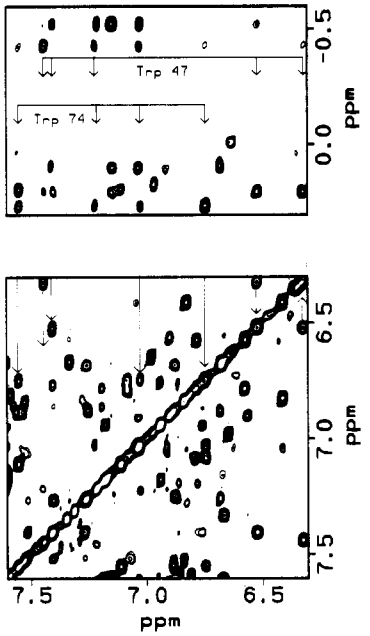

FIGURE 8: Region of a NOESY (100-ms) spectrum of wild-type DHFR in 90% ^1H_2O/10% ^2H_2O showing the aromatic to methyl NOEs (top) and the aromatic–aromatic NOEs (bottom). The most upfield methyl shown in this plot is Val-72 (–0.52 ppm), with NOEs from both Trp-47 ($C^{\zeta 2}H$ and $C^{\eta}H$) and Trp-74 ($C^{\delta}H$ and $C^{\zeta 2}H$). The next methyl (Ile-61 $C^{\delta}H_3$, –0.43 ppm) also has NOEs to Trp-47 ($C^{\delta}H$ and $C^{\zeta 3}H$) and Trp-74 ($C^{\epsilon 3}H$, $C^{\zeta 3}H$, and $C^{\eta}H$). The Ile-61 $C^{\gamma}H_3$ NOEs to Trp-47 and Trp-74 are observed at the bottom of the methyl region of this figure (at 0.27 ppm). The arrows in the aromatic region point to Trp-47 and Trp-74 resonances.

$C^{\eta}H$ belongs to Trp-74 (Figure 7). Distinguishing between these two tryptophans is also possible by noting some of their distinctive NOEs to a Leu/Val spin system (which now can be assigned as Val-72) and to an Ile spin system (which is assigned as Ile-61): the $C^{\delta}H$ of Trp-47 has NOEs to Ile-61 $C^{\delta}H_3$ whereas the $C^{\delta}H$ and $N^{\epsilon}H$ of Trp-74 have NOEs to a $C^{\gamma}H_3$ (–0.52 ppm) of Val-72 (Figure 8). One of the Ile-61 $C^{\gamma}H$ protons is nearly degenerate with its $C^{\delta}H_3$ (see Table I and Figure 9). However, these protons are resolved in several of the site-directed mutants and, thus, can be easily identified with an Ile spin system. The remaining protons of the Ile-61 side chain can be assigned from inspection of the 2QF-COSY spectrum. Figure 9 shows the upfield region of a wild-type

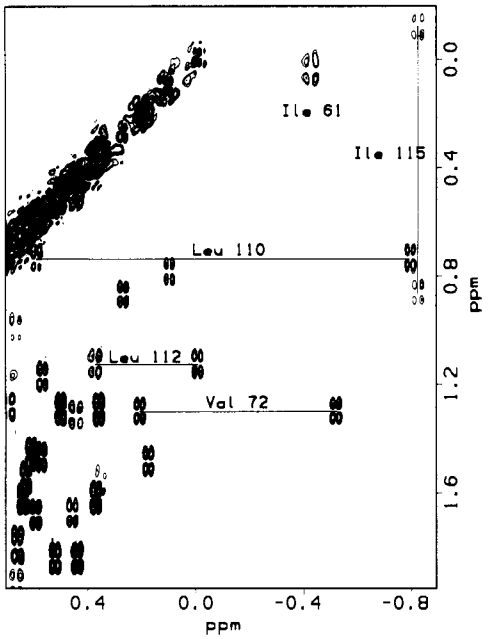

FIGURE 9: Region of a 2QF-COSY spectrum of wild-type DHFR indicating the assignment of the upfield methyl resonances Ile-61, Val-72, Leu-110, Leu-112, and Ile-115.

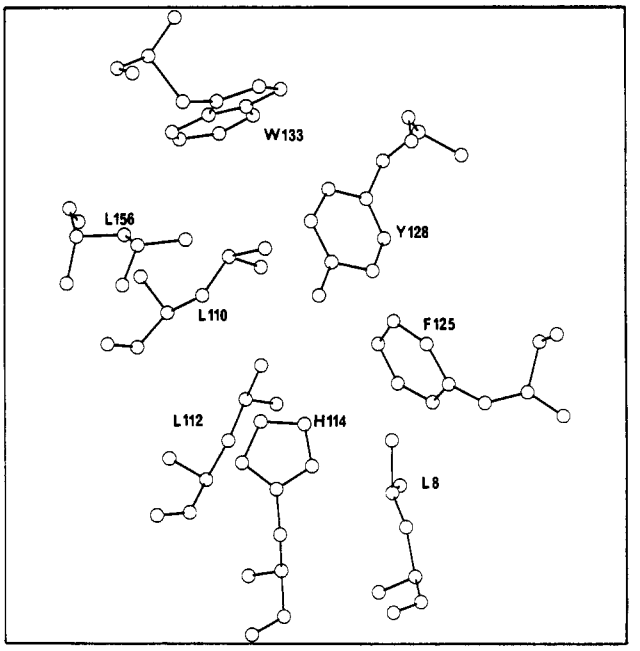

FIGURE 10: Arrangement of the side chains Leu-8, Leu-110, Leu-112, His-114, Phe-125, Tyr-128, Trp-133, and Leu-156 from the X-ray crystal structure of DHFR from *E. coli* (Bolin et al., 1982).

DHFR–folate 2QF-COSY spectrum where these and other assigned spin systems are found.

Phe-125, Tyr-128, Trp-133, His-114, Leu-110, Leu-112, Leu-8, Leu-156, Ala-6, and Ala-107. From the X-ray crystal structure, the aromatic residues Phe-125, Tyr-128, and to a lesser extent Trp-133, should be close to as many as 4 leucines in the βF and βH strands of the β-sheet of DHFR. In particular, Leu-110 is at the center of the three aromatic rings of Phe-125, Tyr-128, and Trp-133, with $C^{\delta}H_3$ to ring proton distances in the 3–4-Å range (Figure 10). Leu-112 is positioned between Phe-125 and Tyr-128, with its methyl groups as close as 3 Å to the Leu-110 methyls. Moving toward the surface of the protein, the Leu-8 methyl groups are directed toward the aromatic rings of Phe-125, Tyr-128, and His-114

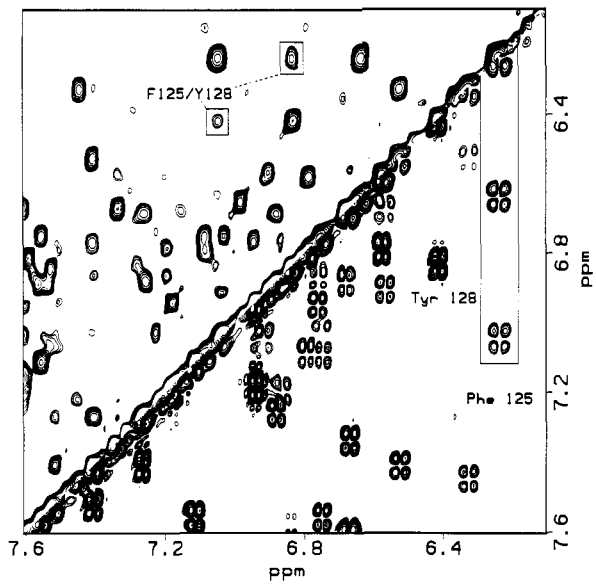

FIGURE 11: Region of a NOESY spectrum (above the diagonal) showing NOEs between Phe-125 and Tyr-128. The spectrum below the diagonal is a 2QF-COSY indicating the assignments for these residues.

and are also close to the methyls of Leu-112. Leu-156 is near to the $C^{\delta}H$ proton of Trp-133 and to Leu-110 and should also show NOEs to His-114. This unique arrangement of hydrophobic residues makes it possible to assign many amino acids in this cluster, located immediately below the nicotinamide binding site.

Strong NOEs are observed between aromatic proton resonances of a phenylalanine ($C^{\delta}H$, 7.04 ppm; $C^{\epsilon}H$, 6.24 ppm; $C^{\zeta}H$, 6.64 ppm) and a tyrosine ($C^{\epsilon}H$, 6.41; $C^{\delta}H$, 6.83 ppm; Figure 11). These two aromatic side chains also exhibit NOE cross peaks to several methyl proton resonances of Leu/Val spin systems. In particular, all ring protons of the tyrosine and the phenylalanine, along with the benzenoid ring protons from a tryptophan ($C^{\epsilon 3}H$, 6.90 ppm; $C^{\zeta 3}H$, 6.57 ppm; $C^{\eta}H$, 6.67 ppm; $C^{\zeta 2}H$, 7.34), have NOEs to an upfield-shifted methyl group resonance at −0.79 ppm. The other methyl of this Leu or Val spin system is at 0.59 ppm and has NOEs to these three aromatic residues as well. Given the uniqueness of this particular arrangement of residues in DHFR, we assign these aromatic amino acids as Phe-125, Tyr-128, and Trp-133. The leucine is probably Leu-110; although there are other leucine residues near both Phe-125 and Tyr-128 in the crystal structure, in particular Leu-112, none are within 5 Å of all three aromatic residues in this cluster. Three leucine spin systems, other than the one assigned as Leu-110, that have interresidue NOEs to either or both Phe-125 and Tyr-128 also exhibit NOEs to a histidine ring. This supports the assignment of Leu-110 ($C^{\delta}H_3$, −0.79, 0.59 ppm; $C^{\gamma}H$, 0.73 ppm), which should not exhibit NOEs to any histidines. This histidine can be assigned as His-114 ($C^{\delta}H$, 6.65 ppm; $C^{\epsilon}H$, 7.65 ppm) on the basis of NOEs to the group of leucines near Phe-125 and Tyr-128.

Phe-125 and Tyr-128 have NOEs to other methyl groups which must comprise the remaining leucines near these residues. The leucine methyls at −0.01 and 0.37 ppm can be assigned to Leu-112 on the basis of interresidue NOEs from Phe-125, Tyr-128, His-114, *and* Leu-110.

The methyl proton resonances at 0.63 and 0.86 ppm can be assigned to Leu-156 on the basis of NOEs to the $C^{\delta}H$ and $C^{\epsilon}H$ protons of Tyr-128, the $C^{\epsilon}H$ of His-114, and the $C^{\delta}H$ of Trp-133. In addition, NOEs are observed to Leu-110 in accord with the crystal structure.

The last leucine side chain to be assigned in this hydrophobic cluster, Leu-8, has methyl proton resonances at 0.36 and 0.50 ppm. This spin system has NOEs to protons of Phe-125, Tyr-128, His-114, and Leu-112. No NOEs are observed to Leu-110, providing a basis for distinguishing this leucine spin system from Leu-112.

The $C^{\zeta 3}H$ and $C^{\eta}H$ protons of Trp-133 and the downfield methyl of Leu-110 have NOEs to an Ala/Thr methyl at 1.80 ppm. NOEs between an Ala/Thr methyl and Leu-110 and, especially, the benzenoid ring of Trp-133 allow assignment of this methyl as Ala-107. In addition, Ala-6 can be assigned on the basis of NOEs to Phe-125 ($C^{\delta}H$, $C^{\epsilon}H$, and $C^{\zeta}H$), the upfield $C^{\delta}H_3$ protons of Leu-112, and both $C^{\delta}H_3$s of Leu-8. Also, in the absence of other Ala/Thr spin systems near these hydrophobic residues, NOEs to an Ala/Thr methyl group resonance identify Ala-6.

Leu-4, Val-93, Phe-103, Ala-81, Val-78, Ile-82, Thr-73, Val-75, and Ser-3. The hydrophobic pocket which extends from Trp-133 contains additional residues in the β-sheet and the E- and F-helices. Near the end of the F-helix is the sole aromatic residue in this region, Phe-103. Hydrophobic side chains surround this aromatic ring. Tyr-100, which is also in the F-helix and remains unassigned at this time, is pointing toward Phe-125 and is not close to most residues in this cluster.

The methyl resonances of a Leu/Val spin system are observed to have NOEs to the $C^{\epsilon}H$ and $C^{\zeta}H$ protons of Phe-125 and to one of the $C^{\delta}H_3$ resonances of Leu-110. NOEs from the CH of this Leu/Val spin system are also observed to this Leu-110 methyl. Both methyls show NOEs to one or both methyls of another Leu/Val spin system (CH_3s, 0.20, 0.72 ppm). The upfield methyl of this second Leu/Val system (at 0.20 ppm) is not degenerate with other spins in this region of the spectrum and has readily identifiable NOEs from this chemical shift. NOEs from Leu-110 *and* Phe-125 to the first Leu/Val spin system ($C^{\delta}H_3$s, 1.00, 1.17 ppm) indicate that this latter system is Leu-4. Leu-4 should show NOEs to Val-93 which we can now assign as the methyls at 0.20 and 0.72 ppm ($C^{\beta}H$, 2.29 ppm).

NOEs between Val-93 and aromatic protons are also observed. Reference to the X-ray crystal structure shows that Val-93 should have NOEs to Phe-103. However, if this aromatic residue is a Phe, its third spin has not been detected in spectra of wild-type or mutant protein. Careful inspection of the rows containing 2QF-COSY cross peaks for this residue reveals that the apparent splitting in ω_2 for the two observable spins is not identical, ruling out the possibility of a Tyr spin system. This aromatic residue must therefore be Phe-103 with either a degenerate or an excessively broadened resonance that is not readily observed. On the basis of the coupling pattern and the observed set of NOEs, it is likely that the protons correspond to the $C^{\delta}H$, $C^{\epsilon}H$, and $C^{\zeta}H$ of Phe-103 at 7.56, 7.12, and 7.12 ppm, respectively.

Many NOEs are observed to the methyl region from Phe-103 and can be used to assign several residues in its environment. One NOE from its $C^{\epsilon}H$ is observed to a methyl belonging to either an Ala or a Thr spin system. Inspection of the X-ray crystal structure reveals that this must be Ala-81 ($C^{\beta}H_3$, 1.70; $C^{\alpha}H$, 3.97 ppm). Phe-103 is also observed to have NOEs to the methyls of a Val(/Leu) spin system ($C^{\gamma}H_3$s, 0.44 and 0.52 ppm; $C^{\beta}H$, 1.84 ppm). The $C^{\alpha}H$ (3.43 ppm) of this spin system is detected in the 2QF-COSY and TOCSY spectra and is found to have NOEs to the $C^{\beta}H_3$ of Ala-81. This residue can be unambiguously assigned as Val-78.

NOEs from the $C^{\epsilon}H$ of Phe-103 to an Ile $C^{\gamma}H$ and $C^{\delta}H_3$ are also observed ($C^{\gamma}Hs$, 1.12 and 2.12 ppm; $C^{\delta}H_3$, 0.96 ppm). One of the methyls belonging to Val-78 (0.44 ppm) has an NOE to the $C^{\delta}H_3$ of this Ile spin system. These NOE connectivities are consistent with the assignment of this residue as Ile-82.

The $C^{\beta}H_3$ of Ala-81 also shows NOEs to both methyls of another Val(/Leu) spin system. These Val(/Leu) methyls also show NOEs to a Thr methyl and $C^{\beta}H$ protons. The 2QF-COSY spectrum reveals the $C^{\alpha}H$ which has an NOE to the $C^{\delta}H$ of Trp-74, making this assignment Thr-73 and the Val(/Leu) side chain with NOEs to Ala-81, Val-75.

A downfield-shifted $C^{\alpha}H$ (6.02 ppm) is found to have NOEs to the methyl resonances of Leu-4 in this hydrophobic pocket, to Tyr-111 ring protons, to the downfield methyl of Leu-110, and to the $C^{\beta}H_3$ of Ala-107. This $C^{\alpha}H$ shows coupling to an NH at 9.45 ppm and is, therefore, not an upfield-shifted amide resonance. One of its $C^{\beta}Hs$ (4.26 ppm) also has NOEs to $C^{\delta}H$ and $C^{\epsilon}H$ or Tyr-111 on the other side of the β-sheet. The other $C^{\beta}H$ resonance cannot be found in this spin system in either TOCSY or 2QF-COSY spectra. However, given its unique complement of NOEs, these protons can only be assigned to Ser-3. This residue is important in that it bridges three hydrophobic clusters where extensive assignments have been made.

Trp-22, His-149, Ile-115, Ala-7, Ala-9, Leu-24, and Thr-113. The assignment of Trp-22 resonances is based on a unique set of NOEs to residues near this important hydrophobic residue. The most upfield-shifted proton resonance of DHFR (−0.82 ppm) belongs to an Ile $C^{\delta}H_3$ (Figure 9). The other resonances of this Ile spin system can be detected in the 2QF-COSY spectrum. An aromatic residue (a Phe or Trp), which is apparently causing the upfield shift, has extensive NOEs to this methyl group. NOEs are observed to a tryptophan $C^{\delta}H$ (identified for all 5 Trp residues in the 90% ^1H_2O/10% ^2H_2O NOESY spectrum) and several other resonances of the benzenoid ring of a tryptophan (Table II). NOEs from the $C^{\delta}H_3$ of this Ile spin system are observed to a methyl group of an Ala/Thr spin system. This Ala/Thr spin system shows NOEs to a Leu/Val spin system *and* to all ring protons of Phe-153. The presence of NOEs to Phe-153 allows assignment of the Ala/Thr resonances as Thr-113 ($C^{\gamma}H_3$, 0.76 ppm; $C^{\beta}H$, 3.92 ppm), the Leu/Val spin system as Leu-24 ($C^{\delta}H$, 0.18, 0.93 ppm; $C^{\gamma}H$, 1.48 ppm), the Ile spin system as Ile-115, and the aromatic proton resonances as Trp-22. Three of the four benzenoid ring protons of Trp-22 are obvious from 2QF-COSY and TOCSY spectra ($C^{\zeta 2}H$, 7.26; $C^{\eta}H$, 6.88; and $C^{\zeta 3}H$, 6.68 ppm). The $C^{\epsilon 3}H$ proton appears to be nearly degenerate with the $C^{\eta}H$ proton and cannot be cleanly assigned at this time from any of the spectra.

A histidine ($C^{\delta}H$, 7.42; $C^{\epsilon}H$, 7.77 ppm) is found to have NOEs to Ile-115 ($C^{\gamma}H_3$), the upfield methyl of Leu-24, and the $C^{\zeta 3}H$ of Trp-22. On the basis of these NOEs, this histidine which resides on the protein surface is assigned as His-149.

Two alanine spin systems in this cluster can be assigned: Ala-7 and Ala-9. The Ala-7 $C^{\beta}H_3$ proton resonance exhibits NOEs to Trp-22 ($N^{\epsilon}H$ and $C^{\zeta 2}H$) and the $C^{\delta}H_3$ of Ile-115. In addition, Ala-7 $C^{\alpha}H$ shows an NOE to the $C^{\beta}H$ of Thr-113. This NOE helps distinguish Ala-7 from Ala-9. The proton resonance of Ala-9 $C^{\beta}H_3$ group shows NOEs to the $C^{\zeta 3}H$ and $C^{\eta}H$ of Trp-22 and only the $C^{\gamma}H_3$ methyl of Ile-115. The $C^{\alpha}H$ of Ala-9 also has an NOE to the $C^{\beta}H$ and $C^{\delta}H_3$ of Ile-115.

Finally, the two remaining histidines, His-45 and His-124, may assigned. His-45 is assigned by observing its disappearance in the spectra of the H45Q mutant and by observing NOEs from its $C^{\delta}H$ to a $C^{\gamma}H_3$ group assigned as Leu-44 ($C^{\gamma}H$, 1.70 ppm; $C^{\delta}H_3$s, 1.03, 1.35 ppm) in the R44L mutant. His-124 is observed to have NOEs to two resonances at 0.82 and 1.02 ppm, which possibly result from Val-13 methyl groups. These methyl resonances cannot be unambiguously assigned due to an incomplete network of NOE connectivities. However, His-124 may be assigned by elimination, the other four His spin systems of DHFR having already been assigned.

Discussion

A major finding stemming from these NMR studies is the absence of multiple forms of the binary complex of *E. coli* DHFR with folate. This is in contrast to the observation by Birdsall et al. (1987) that there are two forms of the corresponding binary complex of *L. casei* DHFR. Two resonances were observed for H7 of the bound pterin ring (at about 8.1 and 9.3 ppm) for the *L. casei* protein at pH 6.8, whereas in the present study a single folate H7 was detected at 9.8 ppm. On the basis of 1D NOE and 1D ROESY spectra (not shown), we estimate that we would detect as little as 5% of a second conformation for the pterin ring if present. In a later paper, Birdsall et al. (1989) argued using NOEs (or their absence) that the two resonances were associated with folate bound to two distinct pterin ring orientations. The first of these, termed the productive form (H7 at 9.3 ppm), has the pterin ring situated for reduction of the N5–C6 imine as required by the previous studies of the stereochemistry of the hydride-transfer step (Charlton et al., 1979). The second form, termed the nonproductive conformation (H7 at 8.3 ppm), is characterized by NOEs between H7 and Leu-19 or Leu-27 (*L. casei* numbering), suggesting that the folate is bound in a conformation similar to that observed for MTX in the X-ray crystal structure of the DHFR–inhibitor complexes (Bolin et al., 1982).

In the present study, we did not detect NOEs to Leu-28 (corresponding to Leu-27 in *L. casei*) but observed NOEs to $C^{\gamma}H_3$ of Ile-5 and $C^{\beta}H$ of Ile-94, both of which are approximately within 4 Å of H7, provided folate is bound in a productive mode. Therefore, the active site of *E. coli* DHFR, despite the striking similarities to *L. casei* in terms of cavity size and the distribution of conserved amino acids, can stabilize only one orientation of the pterin ring in which the N5–C6 imino bond is located appropriately for hydride transfer. NMR investigations of the binary complex of bovine DHFR also indicate formation of a single folate complex (Selinsky et al., 1990).

In summary, on the basis of the X-ray structure and 2D NMR studies of both wild-type and mutant *E. coli* DHFR, we have been able to make self-consistent sequence-specific assignments for over 25% of the amino acid side-chain resonances for the binary folate complex. Use of mutants was particularly important in the assignment process, both for confirming specific assignments and for removing overlaps and ambiguities in the wild-type spectra. Many of these side-chain assignments include the catalytically important residues near or in the active site and thus form the basis of subsequent structural analysis of binary and ternary complexes of wild-type and mutant DHFR with substrate, inhibitors, and the cofactor. Such experiments are in progress and promise to provide new insights into structural changes caused by mutations that result in diminished catalytic activity.

Acknowledgments

We thank our colleagues Drs. J. Cavanagh, W. J. Chazin, H. J. Dyson, J. Moore, M. Rance, N. Skelton, and J. P. Waltho for their helpful discussions. We also thank J. Adams,

P. Jennings, and B. Posner for purifying some of the proteins used in this study. The support of the Penn State NMR facility is also gratefully acknowledged.

References

Baccanari, D. P., Averett, D., Briggs, C., & Burchall, J. (1977) *Biochemistry 16*, 3566–3572.
Benkovic, S. J., Fierke, C. A., & Naylor, A. M. (1988) *Science (Washington, D.C.) 239*, 1105–1110.
Billeter, M., Braun, W., & Wüthrich, K. (1982) *J. Mol. Biol. 155*, 321–346.
Birdsall, B., De Graw, J., Feeney, J., Hammond, S., Searle, M. S., Roberts, G. C. K., Colwell, W. T., & Crase, J. (1987) *FEBS Lett. 217*, 106–110.
Birdsall, B., Feeney, J., Tendler, S. J. B., Hammond, S. J., & Roberts, G. C. K. (1989) *Biochemistry 28*, 2297–2305.
Bodenhausen, G., Vold, R. L., & Vold, R. R. (1980) *J. Magn. Reson. 37*, 93–106.
Bodenhausen, G., Kogler, H., & Ernst, R. R. (1984) *J. Magn. Reson. 58*, 370–388.
Bolin, J. T., Filman, D. J., Matthews, D. A., Hamlin, R. C., & Kraut, J. (1982) *J. Biol. Chem. 257*, 13650–13662.
Bothner-By, A. A., Stephens, R. L., Lee, J., Warren, C. D., & Jeanloz, R. W. (1984) *J. Am. Chem. Soc. 106*, 811–813.
Braunschweiler, L., Bodenhausen, G., & Ernst, R. R. (1983) *Mol. Phys. 48*, 535–560.
Bundi, A., & Wüthrich, K. (1979) *Biopolymers 18*, 285–298.
Charlton, P. A., Young, D. W., Birdsall, B., Feeney, J., & Roberts, G. C. K. (1979) *J. Chem. Soc., Chem. Commun.*, 922–924.
Chen, J.-T., Mayer, R. J., Fierke, C. A., & Benkovic, S. J. (1985) *J. Cell. Biochem. 29*, 73–82.
Chen, J.-T., Taira, K., Tu, C.-P. D., & Benkovic, S. J. (1987) *Biochemistry 26*, 4093–4100.
Dalvit, C., & Wright, P. E. (1987) *J. Mol. Biol. 194*, 313–327.
Davis, D. G. (1989) *J. Magn. Reson. 81*, 603–607.
Fierke, C. A., & Benkovic, S. J. (1989) *Biochemistry 28*, 478–486.
Fierke, C. A., Johnson, K. A., & Benkovic, S. J. (1987) *Biochemistry 26*, 4085–4092.
Kramer, W., Drutsa, V., Jansen, H.-W., Kramer, B., Pflugfelder, M., & Fritz, H.-J. (1984) *Nucleic Acids Res. 12*, 9441–9456.
Marion, D., & Wüthrich, K. (1983) *Biochem. Biophys. Res. Commun. 113*, 967–974.
Murphy, D. J., & Benkovic, S. J. (1989) *Biochemistry 28*, 3025–3031.
Otting, G., Widmer, H., Wagner, G., & Wüthrich, K. (1986) *J. Magn. Reson. 66*, 187–193.
Perry, K. M., Onuffer, J. J., Touchette, N. A., Herndon, C. S., Gittelman, M. S., Matthews, C. R., Chen, J.-T., Mayer, R. J., Taira, K., Benkovic, S. J., Howell, E. E., & Kraut, J. (1987) *Biochemistry 26*, 2674–2682.
Rance, M. (1987) *J. Magn. Reson. 74*, 557–564.
Rance, M., & Wright, P. E. (1986) *J. Magn. Reson. 66*, 372–378.
Rance, M., Sørensen, O. W., Bodenhausen, G., Wagner, G., Ernst, R. R., & Wüthrich, K. (1983) *Biochem. Biophys. Res. Commun. 117*, 479–485.
Sanger, F., Nicklen, S., & Coulson, A. R. (1977) *Proc. Natl. Acad. Sci. U.S.A. 74*, 5463–5467.
Selinsky, B. S., Perlman, M. E., London, R. E., Unkefer, C. J., Mitchell, J., & Blakley, R. L. (1990) *Biochemistry 29*, 1290–1296.

Heterogeneity of Rat Tropoelastin mRNA Revealed by cDNA Cloning[†,‡]

Richard A. Pierce,[§] Susan B. Deak,[§] Catherine A. Stolle,[∥] and Charles D. Boyd*[,§]
Departments of Surgery and Medicine, Robert Wood Johnson Medical School, University of Medicine and Dentistry of New Jersey, New Brunswick, New Jersey 08903-0019

Received March 30, 1990; Revised Manuscript Received July 23, 1990

ABSTRACT: A λgt11 library constructed from poly(A+) RNA isolated from aortic tissue of neonatal rats was screened for rat tropoelastin cDNAs. The first screen, utilizing a human tropoelastin cDNA clone, provided rat tropoelastin cDNAs spanning 2.3 kb of carboxy-terminal coding sequence and extended into the 3′-untranslated region. A subsequent screen using a 5′ rat tropoelastin cDNA clone yielded clones extending into the amino-terminal signal sequence coding region. Sequence analysis of these clones has provided the complete derived amino acid sequence of rat tropoelastin and allowed alignment and comparison with published bovine cDNA sequence. While the overall structure of rat tropoelastin is similar to bovine sequence, numerous substitutions, deletions, and insertions demonstrated considerable heterogeneity between species. In particular, the pentapeptide repeat VPGVG, characteristic of all tropoelastins analyzed to date, is replaced in rat tropoelastin by a repeating pentapeptide, IPGVG. The hexapeptide repeat VGVAPG, the bovine elastin receptor binding peptide, is not encoded by rat tropoelastin cDNAs. Variations in coding sequence between rat tropoelastin cDNA clones were also found which may represent mRNA heterogeneity produced by alternative splicing of the rat tropoelastin pre-mRNA.

Elastin is the major connective tissue protein that confers elasticity to vertebrate elastic tissues (Partridge, 1962; Rosenbloom, 1984). Tropoelastin is the soluble secreted precursor of elastin. In the extracellular space, tropoelastin is extensively cross-linked by the copper-requiring enzyme lysyl oxidase, resulting in an insoluble elastic fiber (Partridge, 1962). The amino acid sequence of tropoelastin was first obtained from tryptic peptides derived from the aortic tissue of copper-deficient pigs. Extensive sequencing of these fragments revealed glycine-rich hydrophobic domains and alanine-rich cross-

[†] This work was supported by NIH Grant HL-42798.
[‡] The nucleic acid sequence in this paper has been submitted to GenBank under Accession Number J05292.
* Address correspondence to this author.
[§] Department of Surgery.
[∥] Department of Medicine.

0006-2960/90/0429-9677$02.50/0